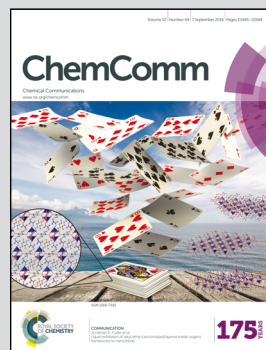


Showcasing research from Tokyo Institute of Technology and Kyushu University, Japan.

Repeatable mechanochemical activation of dynamic covalent bonds in thermoplastic elastomers

Repeated mechanical activation of diarylbibenzofuranone-based mechanophores incorporated in segmented polyurethane elastomers is demonstrated.

As featured in:



See Atsushi Takahara,
Hideyuki Otsuka *et al.*,
Chem. Commun., 2016, 52, 10482.



www.rsc.org/chemcomm

Registered charity number: 207890



Cite this: *Chem. Commun.*, 2016, 52, 10482

Received 7th June 2016,
Accepted 7th July 2016

DOI: 10.1039/c6cc04767j

www.rsc.org/chemcomm

Repeatable mechanochemical activation of dynamic covalent bonds in thermoplastic elastomers†

Keiichi Imato,^{ab} Takeshi Kanehara,^b Shiki Nojima,^b Tomoyuki Ohishi,^c Yuji Higaki,^c Atsushi Takahara^{*bc} and Hideyuki Otsuka^{*a}

Repeated mechanical scission and recombination of dynamic covalent bonds incorporated in segmented polyurethane elastomers are demonstrated by utilizing a diarylbibenzofuranone-based mechanophore and by the design of the segmented polymer structures. The repeated mechanochemical reactions can accompany clear colouration and simultaneous fading.

There is growing interest in mechanochemistry in the field of polymers, because of the fundamental difference between this approach and thermal, electrical and photo-induced polymer reactions.^{1,2} In solution systems, the mechanochemical activation of specific bonds comprised of mechanically sensitive molecules (mechanophores) that are embedded in polymer backbones has facilitated the investigation of forbidden reactions³ and mechanically initiated reactions or polymerizations.^{4–8} Thus, fundamental knowledge about the unique chemistry involved in these reactions can be obtained.^{9–11} Furthermore, single-molecule force spectroscopy has facilitated deeper understanding of such reactions on the molecular scale.^{12,13}

On the other hand, polymer mechanochemistry in bulk systems has provided important mechanistic insights, because of its practical and fascinating applications,^{14–25} such as damage reporting,^{26–29} stress strengthening³⁰ and chemical species release.^{31,32} Previously, however, such behaviours have often been accompanied by material failure or irreversible plastic deformation, which limit further applications of this type of chemistry. Some notable exceptions exist, in which non-scissile, photo-reversible mechanophores are repeatedly activated or irreversible reactions are initiated multiple times.^{20,33–35} However,

repeatable activation of scissile, autonomously regeneratable mechanophores in bulk polymers, which would enable these materials to detect emergent damage^{26–29} and to self-heal small but risk-laden damage,^{36–39} has not yet been reported. Previously, polymeric materials with both damage-detecting and self-healing abilities were developed; however, external stimuli such as UV light irradiation, acid or solvent additives or heating were required in order to initiate damage repair.^{40,41}

Here, we demonstrate the repeated mechanochemical activation and autonomous regeneration (with no external stimuli) of dynamic covalent mechanophores in thermoplastic elastomers. Diarylbibenzofuranone (DABBF) is employed as the mechanophore, which is homolytically cleaved into blue-coloured stable radicals in response to mechanical stress. Further, the generated radicals can recombine autonomously as a result of equilibration at room temperature, where the dissociation ratio is very small (*ca.* 0.001% in solution) (Fig. 1a).^{42–45} Previously, we reported mechanical activation and autonomous recovery of DABBF incorporated in segmented polyurethane elastomers; however, repeated activation was not achieved successfully. This difficulty was most likely due to changes in the molecular aggregation structure caused by stretching.⁴⁶ Therefore, in the present paper, another oligomer with higher molecular mobility, poly(tetramethylene ether glycol) (PTMG), is selected for the soft segment in order to restore the mechanically altered structure.

For the purposes of this study, we designed segmented polyurethane elastomers using DABBF mechanophores incorporated in the soft segments in order to facilitate efficient activation (Fig. 1b).⁴⁶ In these elastomers, the hard segments aggregated to form hard domains *via* strong hydrogen bonding among the urethane linkages, resulting in physical cross-links and elastomeric properties. The elastomers containing DABBF, **P1** and **P2**, were prepared *via* soft pre-polymers composed of dihydroxy DABBF, dihydroxy PTMG (M_n = 1400 for **P1** or 2900 for **P2**) and 4,4'-methylenbis(phenyl isocyanate) (MDI). The subsequent formation of the hard segments was achieved by adding the 1,4-butanediol (BDO) chain extender. The reaction mixtures were homogeneous and gelation was not observed

^a Department of Chemical Science and Engineering, Tokyo Institute of Technology, 2-12-1 Ookayama, Meguro-ku, Tokyo 152-8550, Japan.

E-mail: otsuka@polymer.titech.ac.jp

^b Graduate School of Engineering, Kyushu University, 744 Motoooka, Nishi-ku, Fukuoka 819-0395, Japan

^c Institute for Materials Chemistry and Engineering, Kyushu University, 744 Motoooka, Nishi-ku, Fukuoka 819-0395, Japan

† Electronic supplementary information (ESI) available: Additional synthesis and characterization data. See DOI: 10.1039/c6cc04767j



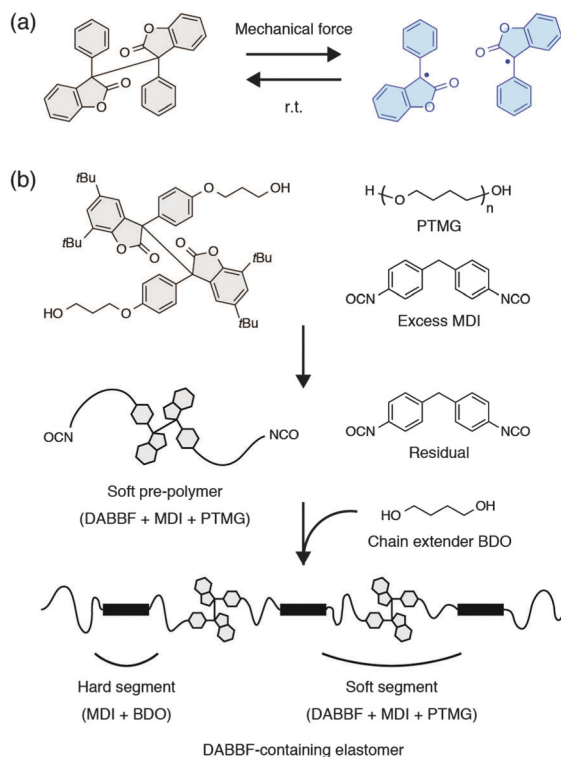


Fig. 1 (a) Mechanically triggered conversion of equilibrium between colourless DABBF and blue-coloured radicals. (b) Scheme for DABBF mechanophore incorporation into segmented polyurethane elastomers.

over the course of the reactions in either case. Further, in the ^1H NMR spectra of the elastomers, each peak could be assigned to the corresponding protons (Fig. S1, ESI †). In the differential scanning calorimetric (DSC) curves of the elastomers, small endothermic peaks originating from melting of the hard segments were observed at 186 and 178 $^\circ\text{C}$ for **P1** and **P2**, respectively (Fig. S2, ESI †). In addition, two glass transitions were observed in each curve, at -88 and 1 $^\circ\text{C}$ for **P1**, and at -58 and 89 $^\circ\text{C}$ for **P2**. The former temperatures (-88 and -58 $^\circ\text{C}$), which are similar to the glass transition temperature (T_g) of PTMG ($T_g = -89$ $^\circ\text{C}$), originate from the soft segments composed of PTMG and MDI, whereas the latter temperatures (1 and 89 $^\circ\text{C}$) originate from other soft segments composed of PTMG, MDI and DABBF. Melting of the PTMG crystallites was observed at 23 $^\circ\text{C}$, in the DSC curve of **P2** only. These results suggest that each elastomer has more than three microphases with different molecular mobility. They also indicate that **P1** is almost amorphous, while **P2** has a crystalline soft segment. This conclusion is also supported by small angle X-ray scattering (SAXS) and wide angle X-ray diffraction (WAXD) measurements of the elastomers (Fig. S3 and S4, ESI †).

Mechanical activation of DABBF units in the elastomers was demonstrated by uniaxial stretching. The **P1** specimen was originally colourless and dumbbell-shaped; however, the colour dramatically changed to blue under manual stretching (Fig. 2a and Movie S1, ESI †). To investigate the activation behaviour at the molecular level, we obtained the *in situ* electron paramagnetic resonance (EPR) spectra during tensile elongation. The g value (2.003) of the spectra indicates that the spectra were

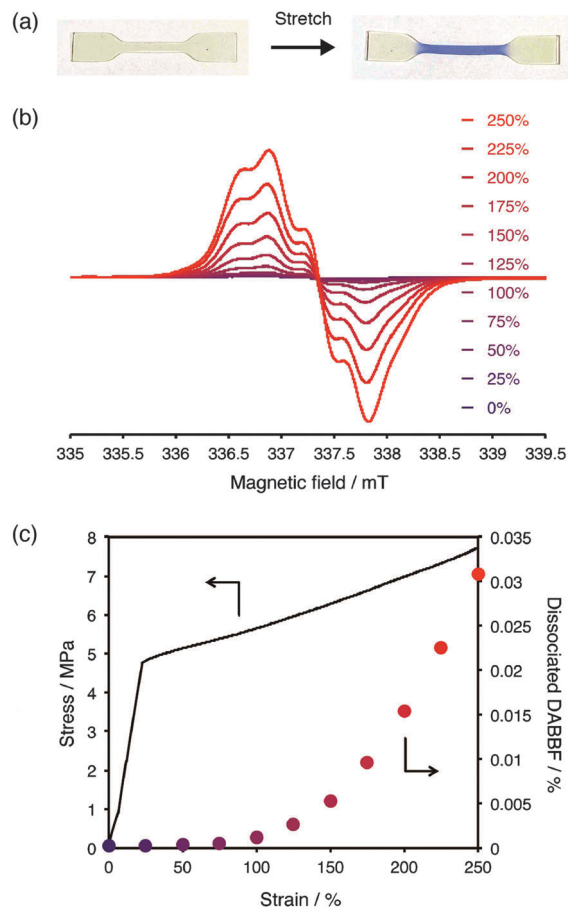


Fig. 2 (a) Photos of manual stretching of dumbbell-shaped DABBF-containing elastomer **P1**. (b) EPR spectra of **P1** as a function of increasing strain. The intensity was normalized by the volume. (c) Part of the typical stress-strain curve of **P1** and the ratio of dissociated DABBF mechanophores in **P1** as a function of the strain.

derived from dissociated DABBF radicals (Fig. 2b).⁴⁴ Small peaks due to the radicals were observed even without strain, because the incorporated mechanophores were in equilibrium at room temperature. The peak intensity began to increase from 100% strain, whereas the spectral shape was unchanged under any strain; this indicates that the mechanical stress cleaved the DABBF mechanophores and produced stable, blue-coloured radicals. Part of the typical stress-strain curve of **P1** and the ratio of dissociated DABBF linkages as a function of the strain are shown together in Fig. 2c. The ratio increased negligibly until 100% strain was achieved, and then increased exponentially to a dissociated ratio of *ca.* 0.03%. Note that it was not possible to measure the ratio at more than 250% strain, because the specimens slipped out of the testing grips. From these results, we concluded that the applied mechanical energy elongated the soft segments with or without DABBF until 100% strain was achieved. Then, energy transfer to the DABBF mechanophores in the soft segment began, which induced the cleavage. We also inferred that the multiple microphases aided activation of the mechanophore. This inference was made because the recombination of the highly mobile radicals, *e.g.*, in a low- T_g



matrix ($T_g = -88\text{ }^{\circ}\text{C}$), was too quick to allow observation of mechanical activation, but the relatively limited mobility of the mechanophore-containing soft domain could suppress the recombination of activated radicals during the elongation.⁴⁵

A clear colouration was also observed in **P2**, under the influence of manual stretching (Fig. S5 and Movie S2, ESI†). That elastomer exhibited higher stress upon uniaxial elongation than that of **P1**, and the dissociation ratio increased almost linearly with strain, indicating a more sensitive response. The higher strength and mechanochromism without an induction period can be attributed to the crystallized PTMG segment, which led to physical cross-links and exclusion of DABBF units from the crystallized domain.

The blue colour of mechanically activated **P1** gradually faded over 6 h at room temperature and eventually disappeared completely, with almost full restoration of the dimensions (Fig. S6, ESI†). Because DABBF equilibrates with a small amount of the corresponding radicals, even at room temperature, and because DABBF was incorporated in the soft segments with T_g below room temperature, the mechanical stress biased the equilibrium towards the dissociated side temporarily. The equilibrium then returned to the initial state gradually in the absence of stress, generating transient activation (colouration) and autonomous recombination. A clear colouration was also observed in **P1** via second and third stretching (Movie S3, ESI†). To inspect this repeated activation, EPR spectra were measured under constant strains of 50% (without slack) and 200% in each cycle. The spectral intensity was largely unchanged throughout the cycling (Fig. 3a). The dissociation ratio upon each stretching is shown in Fig. 3b; the second and third elongation generated as many

radicals as the first elongation. This repeated activation was most likely due to the high molecular motion of the PTMG chains and the resulting restoration of the altered molecular aggregation structure. Indeed, the stress-strain curve profiles obtained for the cyclic tensile tests were almost unchanged, while large hysteresis and a slight decrease in the stress were observed (Fig. 3c). In addition, strain-induced crystallization of the PTMG chains was not observed in the WAXD measurements (Fig. S7, ESI†). On the other hand, **P2** also exhibited repeated activation, but the dissociation ratio decreased gradually with cycling (Fig. S8, ESI†). This is most likely because the molecular aggregation structure was changed significantly, *e.g.*, through fragmentation of the PTMG crystalline domains and strain-induced crystallization of the PTMG chains, as indicated by the results of the cyclic tensile test (Fig. S8, ESI†).

A plausible mechanism for the repeated mechanochemical activation and autonomous regeneration of DABBF mechanophores in **P1** is shown in Fig. 3d. The applied tensile stress elongated the soft segments first until 100% strain was achieved. After the soft segments were fully extended, the DABBF mechanophores began to dissociate. In these processes, the aggregated hard domains functioned as physical cross-links and were only slightly dissociated, and the strain did not induce crystallization of the PTMG soft segments. Following removal of the stress, the extended chains were restored by the entropic elasticity and, during the restoration process, the activated radicals gradually recombined. Therefore, the elastomer exhibited good repeatability as regards the mechanical properties and DABBF activation.

In this study, repeated mechanical activation and regeneration of DABBF dynamic covalent mechanophores were demonstrated

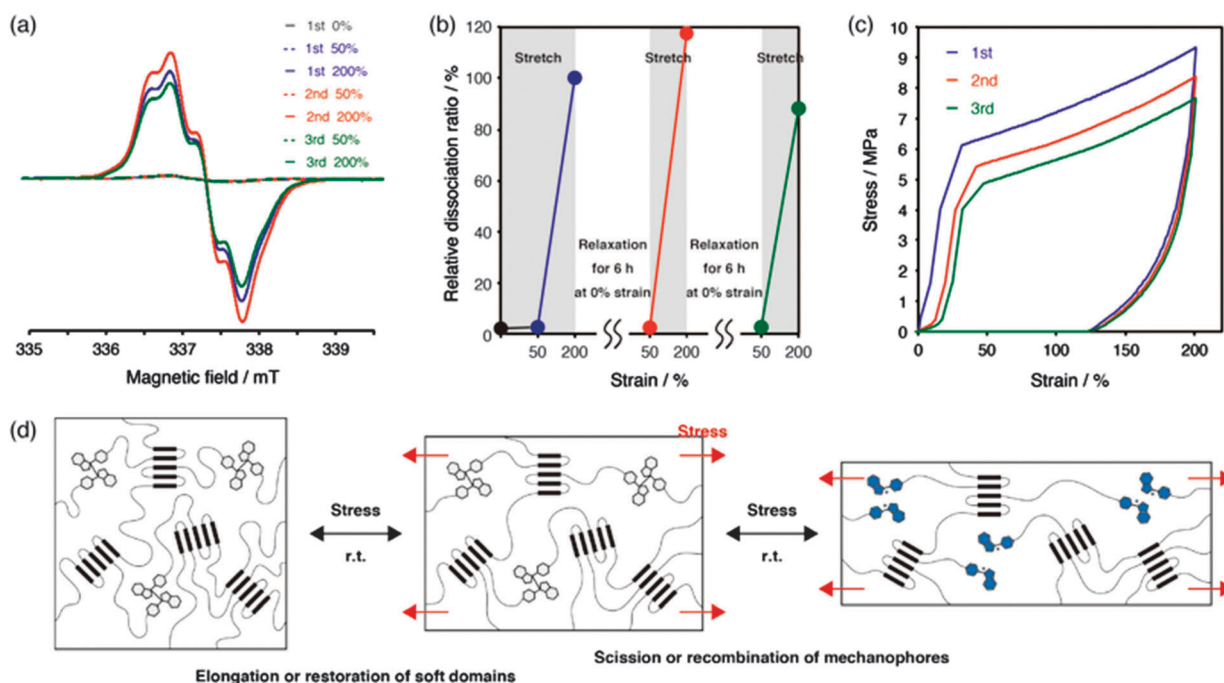


Fig. 3 (a) EPR spectra for repeated activation of DABBF mechanophores in **P1**, which was elongated to 50% and 200% strain and relaxed for 6 h at 0% strain. The intensity was normalized by the volume. (b) Ratio of dissociated mechanophores in **P1** for repeated activation. (c) Cyclic stress-strain curves of **P1**. (d) Proposed mechanism for repeated mechanical activation and autonomous regeneration of **P1**.



for segmented polyurethane elastomers. The high molecular mobility of non-crystalline PTMG at room temperature restored the mechanically changed polymer structures, which enabled repeated mechanical activation. This is the first report of repeatable activation of scissile, autonomously regeneratable mechanophores in bulk polymers. We believe that this reversible mechanochromism could facilitate the realization of an ideal material with the ability to signal emergent damage and to self-heal potentially dangerous damage, which could be applied in various fields. In particular, such a material would have considerable applications in scenarios where real-time, reversible detection of small mechanical forces is desired.

H. O. gratefully acknowledges financial support from KAKENHI (No. 26288057 and 26620175). This work was also supported by the NEXT Program (No. GR077) and the ImPACT Program from Council for Science, Technology and Innovation (Cabinet Office, Government of Japan) and by the Photon and Quantum Basic Research Coordinated Development Program from MEXT, Japan. The synchrotron radiation experiments were performed at BL40B2 (2014A1249) in SPring-8 with the approval of the Japan Synchrotron Radiation Research Institute (JASRI).

Notes and references

- 1 M. M. Caruso, D. A. Davis, Q. Shen, S. A. Odom, N. R. Sottos, S. R. White and J. S. Moore, *Chem. Rev.*, 2009, **109**, 5755.
- 2 J. Li, C. Nagamani and J. S. Moore, *Acc. Chem. Res.*, 2015, **48**, 2181.
- 3 C. R. Hickenboth, J. S. Moore, S. R. White, N. R. Sottos, J. Baudry and S. R. Wilson, *Nature*, 2007, **446**, 423.
- 4 A. Piermattei, S. Karthikeyan and R. P. Sijbesma, *Nat. Chem.*, 2009, **1**, 133.
- 5 J. M. Lenhardt, A. L. Black and S. L. Craig, *J. Am. Chem. Soc.*, 2009, **131**, 10818.
- 6 M. J. Kryger, M. T. Ong, S. A. Odom, N. R. Sottos, S. R. White, T. J. Martínez and J. S. Moore, *J. Am. Chem. Soc.*, 2010, **132**, 4558.
- 7 C. E. Diesendruck, G. I. Peterson, H. J. Kulik, J. A. Kaitz, B. D. Mar, P. A. May, S. R. White, T. J. Martínez, A. J. Boydston and J. S. Moore, *Nat. Chem.*, 2014, **6**, 623.
- 8 M. J. Robb and J. S. Moore, *J. Am. Chem. Soc.*, 2015, **137**, 10946.
- 9 D. C. Church, G. I. Peterson and A. J. Boydston, *ACS Macro Lett.*, 2014, **3**, 648.
- 10 J. Li, T. Shiraki, B. Hu, R. A. E. Wright, B. Zhao and J. S. Moore, *J. Am. Chem. Soc.*, 2014, **136**, 15925.
- 11 B. Lee, Z. Niu, J. Wang, C. Sledobnick and S. L. Craig, *J. Am. Chem. Soc.*, 2015, **137**, 10826.
- 12 H. M. Klukovich, T. B. Kouznetsova, Z. S. Kean, J. M. Lenhardt and S. L. Craig, *Nat. Chem.*, 2013, **5**, 110.
- 13 J. Wang, T. B. Kouznetsova, Z. Niu, M. T. Ong, H. M. Klukovich, A. L. Rheingold, T. J. Martínez and S. L. Craig, *Nat. Chem.*, 2015, **7**, 323.
- 14 C. K. Lee, D. A. Davis, S. R. White, J. S. Moore, N. R. Sottos and P. V. Braun, *J. Am. Chem. Soc.*, 2010, **132**, 16107.
- 15 C. M. Kingsbury, P. A. May, D. A. Davis, S. R. White, J. S. Moore and N. R. Sottos, *J. Mater. Chem.*, 2011, **21**, 8381.
- 16 B. A. Beiermann, D. A. Davis, S. L. B. Kramer, J. S. Moore, N. R. Sottos and S. R. White, *J. Mater. Chem.*, 2011, **21**, 8443.
- 17 J. M. Lenhardt, A. L. Black, B. A. Beiermann, B. D. Steinberg, F. Rahman, T. Samborski, J. Elsakar, J. S. Moore, N. R. Sottos and S. L. Craig, *J. Mater. Chem.*, 2011, **21**, 8454.
- 18 A. L. Black, J. A. Orlicki and S. L. Craig, *J. Mater. Chem.*, 2011, **21**, 8460.
- 19 B. A. Beiermann, S. L. B. Kramer, J. S. Moore, S. R. White and N. R. Sottos, *ACS Macro Lett.*, 2012, **1**, 163.
- 20 H. T. Baytekin, B. Baytekin and B. A. Grzybowski, *Angew. Chem., Int. Ed.*, 2012, **51**, 3596.
- 21 C. K. Lee, B. A. Beiermann, M. N. Silberstein, J. Wang, J. S. Moore, N. R. Sottos and P. V. Braun, *Macromolecules*, 2013, **46**, 3746.
- 22 C. M. Degen, P. A. May, J. S. Moore, S. R. White and N. R. Sottos, *Macromolecules*, 2013, **46**, 8917.
- 23 B. A. Beiermann, S. L. B. Kramer, P. A. May, J. S. Moore, S. R. White and N. R. Sottos, *Adv. Funct. Mater.*, 2014, **24**, 1529.
- 24 B. Baytekin, H. T. Baytekin and B. A. Grzybowski, *Angew. Chem., Int. Ed.*, 2014, **53**, 6946.
- 25 J. W. Kim, Y. Jung, G. W. Coates and M. N. Silberstein, *Macromolecules*, 2015, **48**, 1335.
- 26 D. A. Davis, A. Hamilton, J. Yang, L. D. Cremer, D. Van Gough, S. L. Potisek, M. T. Ong, P. V. Braun, T. J. Martínez, S. R. White, J. S. Moore and N. R. Sottos, *Nature*, 2009, **459**, 68.
- 27 Y. Chen, A. J. H. Spiering, S. Karthikeyan, G. W. M. Peters, E. W. Meijer and R. P. Sijbesma, *Nat. Chem.*, 2012, **4**, 559.
- 28 D. W. R. Balkenende, S. Coulibaly, S. Balog, Y. C. Simon, G. L. Fiore and C. Weder, *J. Am. Chem. Soc.*, 2014, **136**, 10493.
- 29 R. Göstl and R. P. Sijbesma, *Chem. Sci.*, 2016, **7**, 370.
- 30 A. L. B. Ramirez, Z. S. Kean, J. A. Orlicki, M. Champhekar, S. M. Elsakar, W. E. Krause and S. L. Craig, *Nat. Chem.*, 2013, **5**, 757.
- 31 C. E. Diesendruck, B. D. Steinberg, N. Sugai, M. N. Silberstein, N. R. Sottos, S. R. White, P. V. Braun and J. S. Moore, *J. Am. Chem. Soc.*, 2012, **134**, 12446.
- 32 M. B. Larsen and A. J. Boydston, *J. Am. Chem. Soc.*, 2013, **135**, 8189.
- 33 R. T. M. Jakobs, S. Ma and R. P. Sijbesma, *ACS Macro Lett.*, 2013, **2**, 613.
- 34 M. B. Larsen and A. J. Boydston, *J. Am. Chem. Soc.*, 2014, **136**, 1276.
- 35 G. R. Gossweiler, G. B. Hewage, G. Soriano, Q. Wang, G. W. Welshofer, X. Zhao and S. L. Craig, *ACS Macro Lett.*, 2014, **3**, 216.
- 36 P. Cordier, F. Tournilhac, C. Soulié-Ziakovic and L. Leibler, *Nature*, 2008, **451**, 977.
- 37 G. H. Deng, C. M. Tang, F. Y. Li, H. F. Jiang and Y. M. Chen, *Macromolecules*, 2010, **43**, 1191.
- 38 Y. Chen, A. M. Kushner, G. A. Williams and Z. Guan, *Nat. Chem.*, 2012, **4**, 467.
- 39 H. Ying, Y. Zhang and J. Cheng, *Nat. Commun.*, 2014, **5**, 3218.
- 40 D. Ramachandran, F. Liu and M. W. Urban, *RSC Adv.*, 2012, **2**, 135.
- 41 G. Hong, H. Zhang, Y. Lin, Y. Chen, Y. Xu, W. Weng and H. Xia, *Macromolecules*, 2013, **46**, 8649.
- 42 K. Imato, M. Nishihara, T. Kanehara, Y. Amamoto, A. Takahara and H. Otsuka, *Angew. Chem., Int. Ed.*, 2012, **51**, 1138.
- 43 K. Imato, T. Ohishi, M. Nishihara, A. Takahara and H. Otsuka, *J. Am. Chem. Soc.*, 2014, **136**, 11839.
- 44 K. Imato, A. Irie, T. Kosuge, T. Ohishi, M. Nishihara, A. Takahara and H. Otsuka, *Angew. Chem., Int. Ed.*, 2015, **54**, 6168.
- 45 K. Imato, A. Takahara and H. Otsuka, *Macromolecules*, 2015, **48**, 5632.
- 46 K. Imato, T. Kanehara, T. Ohishi, M. Nishihara, H. Yajima, M. Ito, A. Takahara and H. Otsuka, *ACS Macro Lett.*, 2015, **4**, 1307.

